

Fig.3 Schematic of equatorial thermocline displacements involving (a) an adiabatic, horizontal redistribution of warm surface waters (left panel) as occurs during the oscillation between El Niño and La Niña; and (b) diabatic changes in thermocline that can induce El Padre (or permanent El Niño) when the thermocline is deep, and La Madre conditions when the thermocline is shallow.

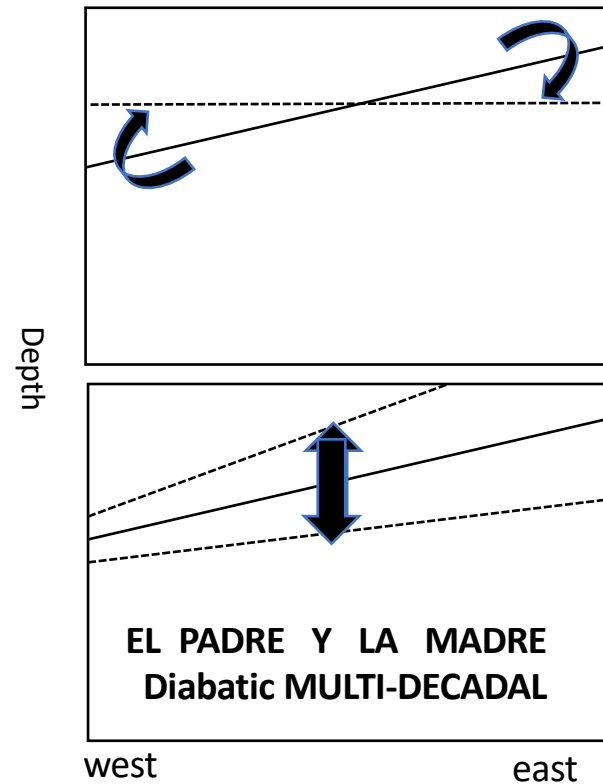


Fig.4 Schematic of the two main components of the meridional ocean circulation. The red region denotes the domain of the wind-driven circulation, which involves upwelling at the equator, poleward Ekman drift, and subduction in the subtropics with a return flow in the upper 200 m. In the Atlantic the thermohaline circulation has both an upper branch with waters subducting in the far north, travelling southward, and upwelling in the Southern Ocean (*light blue*), and a lower branch with waters downwelling in the southern polar region (*dark blue*).

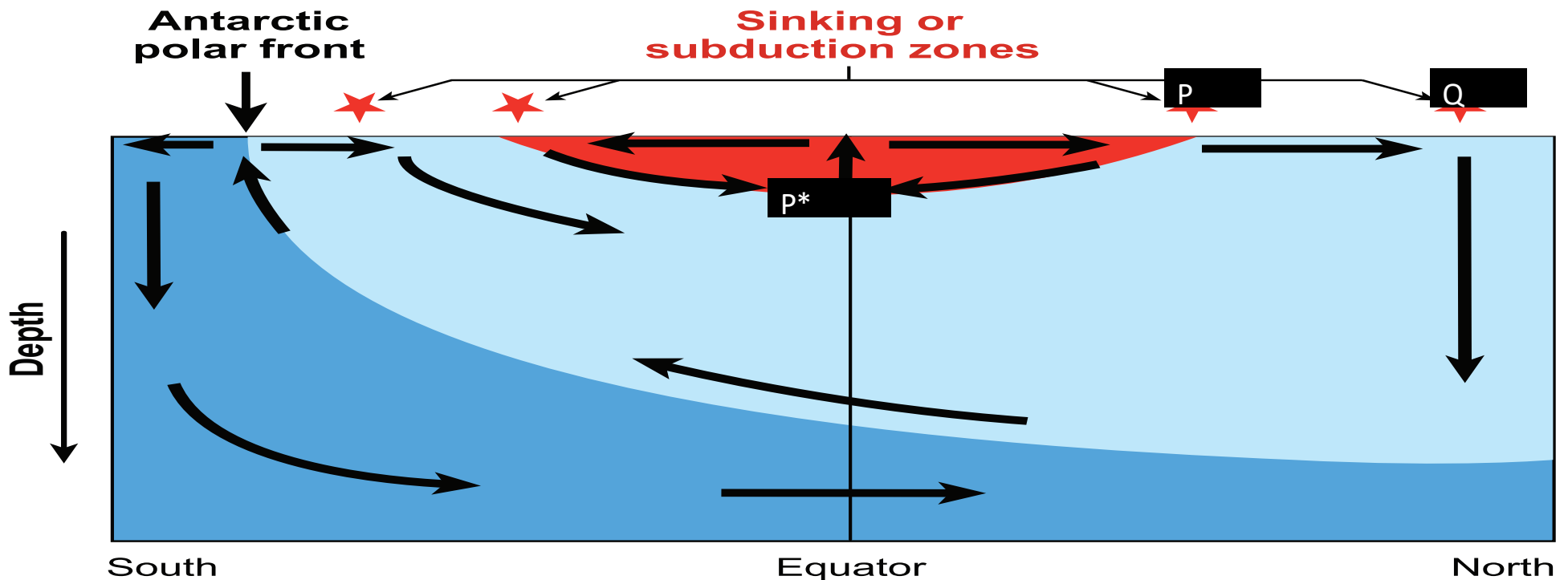
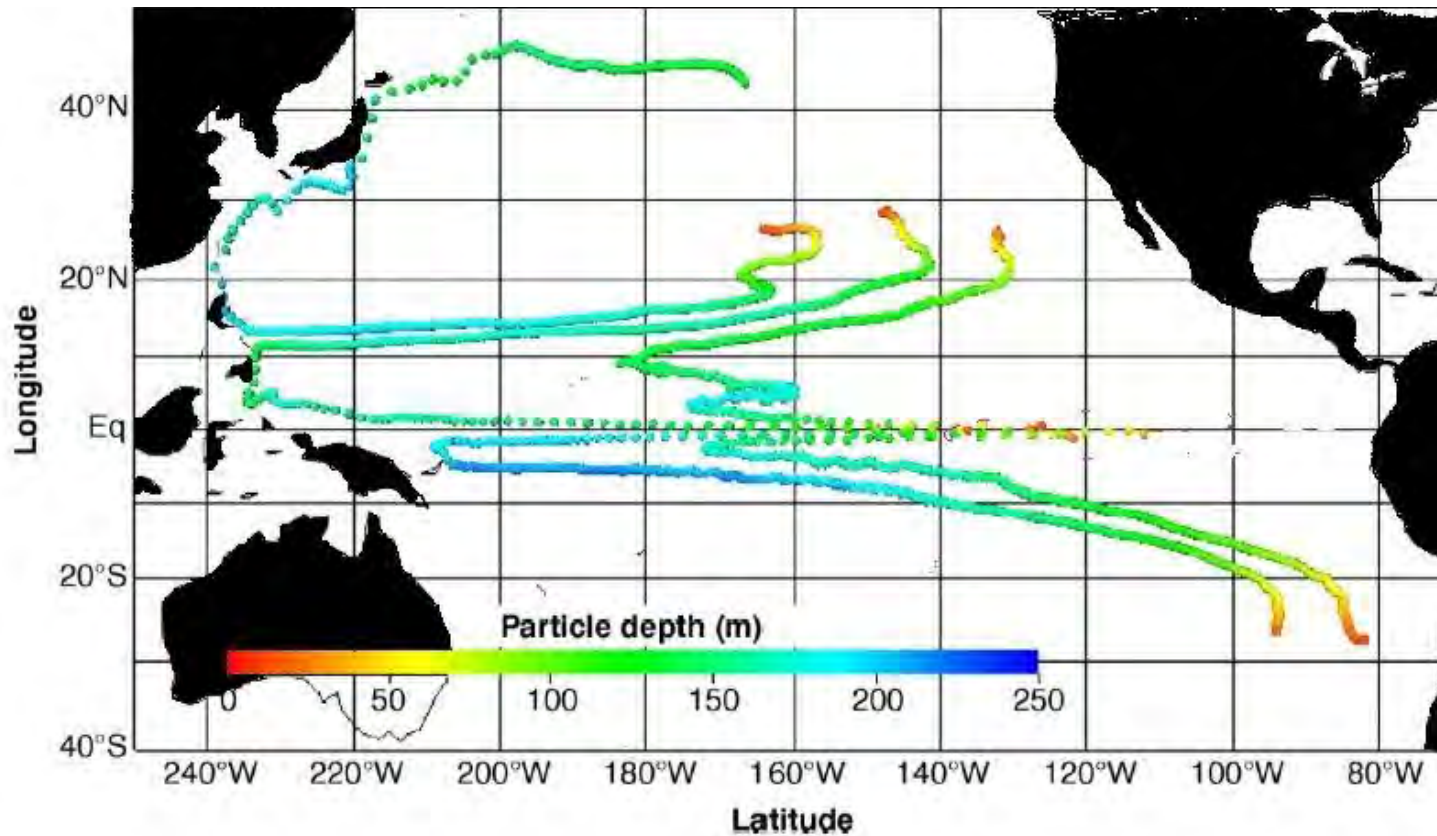


Fig. 5. The tropical wind-driven circulation. The paths of water parcels over a period of 16 years after subduction off the coasts of California and Peru as simulated by means of a realistic oceanic general circulation model forced with the observed climatological winds.



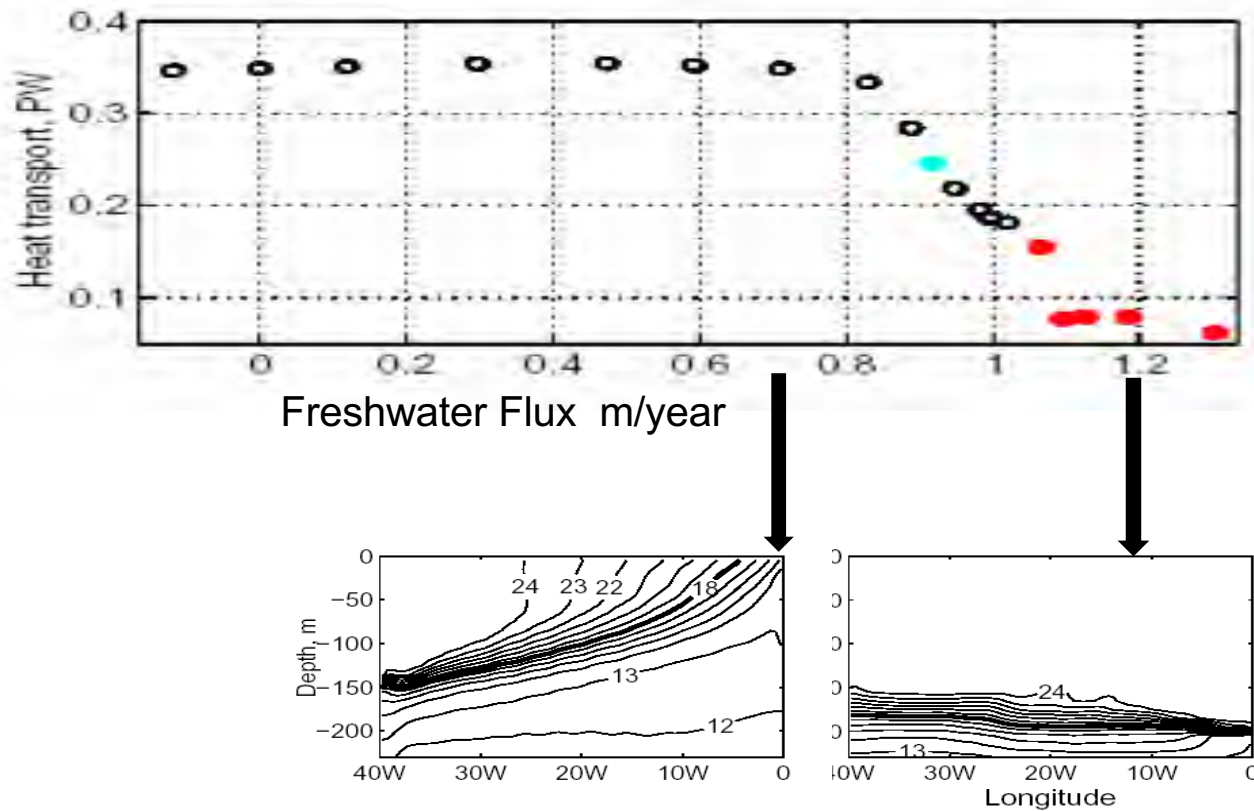


FIG. 6 Changes in the meridional oceanic heat transport (in petawatts) across a fixed latitude of an idealized model ocean as the flux of fresh water onto the ocean surface increases. That flux measures only precipitation, but evaporation minus precipitation is such that the mean salinity of the surface remains constant. The vertical dashed black lines represent the effect of changes in the mean salinity on the “cliff” between La Madre and El Padre conditions. An increase in mean salinity facilitates a transition to El Padre, causing the dashed black line to move to the left.

The bottom panels show the thermal structure in the equatorial plane when El Padre prevails at point A (right panel) and when La Madre prevails at B (left panel). For details see (14).

Fig 7 (Top) SST records in the western equatorial Pacific (red line, ODP site 806) and in the eastern equatorial Pacific (blue line, site 847), both based on Mg/Ca, and that for the eastern Pacific based on alkenones (green dots, site 847). Larger circles are for the data based on Mg/Ca but from ODP sites 806 (red) and 847 (blue). Pink shading denotes the early Pliocene. (Bottom) Alkenone-based SST records for the California margin (black, ODP site 1014), the Peru margin (blue, site 1237), and the West African margin (green) site 1084.

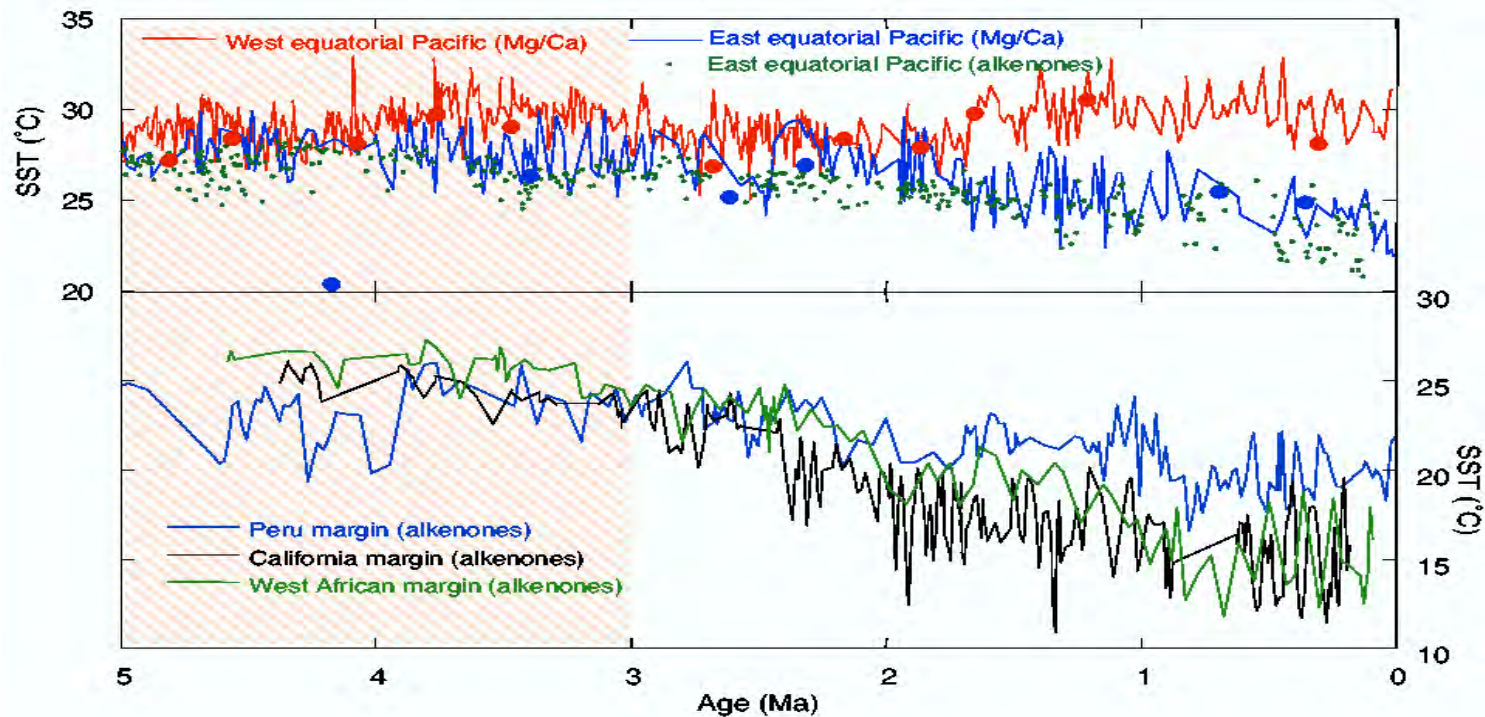


Fig.8 A composite record from caves in southern China of variations in $\delta^{18}O$ that provide a measure of rainfall in the area (16). The values of $\delta^{18}O$ are offset by 8.5‰. (b) Sea surface temperature record from the eastern equatorial Pacific (15). (c) Benthic oxygen isotope record, a measure of global ice volume (2). (d) Normalized insolation at 00N, on June 21 (red) and obliquity (black). In (a), (b), and (c) normalized insolation at 00N on June 21 is plotted for reference. Time series in (b) and (c) have been normalized.

